 doi:10.20944/preprints201812.0336.v1

Molecular docking and molecular dynamics (MD) simulation of human anti complement factor H (CFH) antibody Ab42 and CFH polypeptide (pCFH)

Bing Yang[1,2†], Jiayi Ren[3†], Tong Liu[1,2], Shujian Lin[1,2], Yueming Wang[1,4], Chengming Li[1,4], Youwen He[1,4], Wenwen Xu[1,5], Weihong Zheng[5], Xiaohui Yuan[1,5*], Huaxin Liao[1,5*]

1. Institute of Biomedicine, Jinan University, Guangzhou, 510632, China;
2. Guangdong Provincial Key Laboratory of Bioengineering Medicine, Guangzhou, 510632, China;
3. Zhuhai College of Jilin University, Zhuhai, 519041, China;
4. National Engineering Research Center of Genetic Medicine, Guangzhou, 510632, China;
5. Zhuhai Trinomab Biotechnology Co., Ltd. Zhuhai, 519040, China;

†These authors contribute equally to this work.

*Corresponding to Yuan Xiaohui (yuanhui1024@gmail.com) and Liao Huaxin (larryhliao@163.com).

 doi:10.20944/preprints201812.0336.v1

Abstract

The details of antigen-antibody interactions and the identification of epitopes are critical for the development of monoclonal antibody drugs. Ab42 is a native human-derived anti-CFH monoclonal antibody. In this study, the interaction between antigen pCFH and antibody (Ab42) was theoretically demonstrated by molecular docking and MD simulation, combined with free energy calculation and computational alanine scanning (CAS), and key amino acids and epitopes were identified. Experimental alanine scanning (EAS) was then carried out to verify the results of the calculation, and our results indicated that Ab42 antibody forms hydrogen bonds and interacts hydrophobically with pCFH through the Tyr315, Ser100, Gly33, and Tyr53 residues on its CDR, while the main pCFH epitopes are located at the six sites of Pro441, Ile442, Asp443, Asn444, Ile447, and Thr448. In conclusion, this study has explored the mechanism of antigen-antibody interaction from both theoretical and experimental aspects, and our results have important theoretical significance for the design and development of relevant antibody drugs.

Keywords: Complement factor H (CFH), Molecular docking, Molecular dynamics (MD) simulation, Computational alanine scanning (CAS), Experimental Alanine Scanning (EAS)

 doi:10.20944/preprints201812.0336.v1

Introduction

CFH is a soluble glycoprotein expressed by normal epidermal cells with a molecular weight of 155 kDa[1,2]. The main function of CFH is to protect the host cells from complement system-mediated attack and destruction through inhibiting the complement activation pathway, i.e., preventing the deposition of C3b on the surface of target cells[3,4]. Certain malignant tumor cells escape the body's tumor clearance through over-expressing CFH, which is one of the important mechanisms of malignant tumors escaping the immunity[3,5].

The polypeptide domain SCR19 on the CFH protein (sequence: GPPPPIDNGDITSFP) is an important region for its binding to the membrane of C3b-expressing cells[2,5]. Previous literature also reported that anti-pCFH antibodies recognize and bind CFH on the surface of tumor cells and thereby facilitate the activation of complement system, which in turn damages the tumor cells by both complement-dependent cytotoxicity (CDC) and antibody-dependent complement-mediated cytotoxicity (ADCC) and ultimately suppresses tumor growth and preventing tumor metastasis[6,7].

Ab42 is an human-derived high-affinity anti-pCFH monoclonal antibody isolated previously in our laboratory from the peripheral blood mononuclear cells of a malignant glioma patient using a single memory B lymphocyte sorting and RT-PCR method [8]. As a native human antibody, it can avoid the immune rejection of the body and thus has an important application prospect for the development of anti-tumor drugs.

Preprints (www.preprints.org) | NOT PEER-REVIEWED | Posted: 28 December 2018 doi:10.20944/preprints201812.0336.v1

Information on the interaction of antibodies with their targets is critical for the development of antibody drugs. Molecular docking[9,10] and MD simulation[11,12] methods provide an advantageous means for studying the interaction between antigen and antibody. Our previous studies have screened different solvent water models and force field calculations in the MD simulation system and suggested that amber99sb_spce is the best candidate model for studying antigen-antibody interactions[13].

Therefore, the present work applied this amber99sb_spce model to study the interaction between Ab42 antibody and pCFH by molecular docking, MD simulation, and CAS[14,15], and successfully identified the binding epitope of Ab42. Finally, the results of theoretical calculations were further verified by both EAS[1,16] and enzyme-linked immunosorbent assay (ELISA) antigen-antibody binding experiments.

Results and Discussion

The three-dimensional (3D) structure of Ab42

Ab42 was originally an intact antibody containing FC segment. However, in the calculation part of this work, in order to more accurately describe the interaction between the antigen and the antibody and simplify the calculation, only the Fab segment of Ab42 antibody was established (Figure 1A). We used the Verify Protein (Profiles-3D) program under the Homology Modeling module to examine the compatibility scores of each amino acid residue in its primary sequence on both the homology modeled structure and the corresponding 3D spatial structure.

Preprints (www.preprints.org) | NOT PEER-REVIEWED | Posted: 28 December 2018 doi:10.20944/preprints201812.0336.v1

Figure 1B shows that the Verify Score of Ab42 antibody structure is greater than zero, indicating that the amino acid sequence of Ab42 antibody is compatible with its corresponding 3D structure. The stereo-chemical accuracy of the model, including the rationality of structural parameters, such as bond length, bond angle, and dihedral angle, was evaluated by the Ramachandran plot analysis method, which shows that most of the atoms are located in the first quadrant, second quadrant, and third quadrant, demonstrating that the bond lengths, bond angles, and dihedral angles of the entire molecule are reasonable (Figure 1C). These results are similar to the template for homology modeling and are also consistent with the Profiles-3D predictions, suggesting that the structure of Ab42 antibody was precisely optimized by energy minimization with correct stereo-structure accuracy.

Molecular docking

The ZDOCK program was used to perform the molecular docking between pCFH and Ab42 proteins to achieve the highest docking pose (Figure 2). Our results showed that the entire pCFH molecule spans around the CDR of Ab42 molecule (Figure 2A), and subsequent analysis further revealed that pCFH interacts strongly with the surface amino acids of Ab42, mainly by hydrogen bonding and hydrophobic interaction (Figure 2B), which play the major roles in the binding of pCFH to Ab42 antibody. As shown in Figure 2B, pCFH forms hydrogen bonds with the sites of Tyr315, Ala103, Ser100, Gly33, Ser52, and Leu31 on the CDR of Ab42 antibody, and interacts hydrophobically with the sites of Tyr248, Tyr255, and Ala104 too.

In the docking model, 15 intermolecular hydrogen bonds were formed in the

Preprints (www.preprints.org) | NOT PEER-REVIEWED | Posted: 28 December 2018 doi:10.20944/preprints201812.0336.v1

Ab42-pCFH complex (Table 2) with an average length of approximately 2.0 angstroms, indicating that they play the most important roles in the binding between Ab42 and pCFH during the complex formation, followed by the hydrophobic interactions.

Stability analysis of Ab42-pCFH complex

MD simulation can be used to solve the energy barrier problem that EM calculation cannot overcome, and the equilibrium trajectory of MD can be used for the conformation sampling of MM-PBSA combined with free energy calculation. In this study, the Ab42-pCFH complex was subjected to three MD simulations under the force field of Amber99sb-spce with each run lasting 100 ns (designated as MD-1, MD-2, and MD-3, respectively), and the root mean square deviations (RMSDs) were analyzed subsequently to evaluate the balance of trajectory.

As shown in Figure 3A, the three MD repeats obtained similar MD trajectories, and the system reached equilibrium at approximately 40 ns. Since the interaction of antigen and antibody is mainly between the epitope of the antigen and the CDR of the antibody, in the RMSD analysis, we used the index tool of gromacs (Make_ndx) to define the CDR of Ab42 and the pCFH as a molecular group. In the 100 ns MD process, in addition to analyze the RMSD of the total backbone, the variation curve of CDR-pCFH was also analyzed (Figure 3B). The antibody CDR interacted with the pCFH, and the results of RMSD analysis of the CDR-pCFH group showed that the RMSD values remained within the range of 0.1 nm, indicating that the CDR regions of the antibody maintained a stable binding state with pCFH.

Preprints (www.preprints.org) | NOT PEER-REVIEWED | Posted: 28 December 2018 doi:10.20944/preprints201812.0336.v1

MM-PBSA and energy decomposition

In order to further explore the interaction mechanism between pCFH and its antibody Ab42, the equilibrium phase of the three kinetic simulation of the Ab42-pCFH complex structure was selected and sampled. Binding free energy and residue decomposition were then calculated using MM-PBSA. As shown in Table 3, the binding free energies MD-1, MD-2, and MD-3 obtained from the three MD simulations were -608.996±55.221 KJ/mol, -626.732±65.203 KJ/mol, and -658.252± 66.766 KJ/mol, respectively. During the interaction between pCFH antigen and Ab42 antibody, the electrostatic interaction, van der Waals force, and non-polar solvation play important roles combinatorially.

Taking average of the residual energy contribution values obtained from the three simulations, we further analyzed the energy contributions of pCFH and the key amino acid sites on the CDR of Ab42 separately, and the results showed that almost all the amino acids in pCFH sequence (except for GLY437 and GLY445, which did not interact with the antibody), displayed negative energy values (i.e., PRO441, ILE442, ASP-443, ASP-446, ILE-447, THR448, and PRO451), strongly demonstrating that these amino acids on the polypeptide facilitate the binding of Ab42-pCFH, whereas the two sites of GLY437 and GLY445 may exert an adverse effect on the antigen-antibody interaction.

Comparison of CAS and EAS

Alanine mutation of an amino acid replaces its reactive group with a small neutral methyl group on the side chain, exerting little effect on the whole protein

Preprints (www.preprints.org) | NOT PEER-REVIEWED | Posted: 28 December 2018 doi:10.20944/preprints201812.0336.v1

structure, and hence is commonly used in observing the functional impact of amino acids on proteins. Therefore, this study used alanine mutation to further verify the results of CAS by performing EAS on the interaction of Ab42 with pCFH.

The free energy changes after amino acid mutation into alanine were mainly considered in the CAS. An energy value of >0.5 Kcal/mol after the mutation indicates that the structure is unstable and that the particular amino acid *in situ* plays an important role in stabilizing the structure, whereas an post-mutational energy value of <-0.5 Kcal/mol means that the structure remains stable and that the original amino acid *in situ* is not conducive to the structural stability; similarly, a mutation energy between 0.5 and -0.5 Kcal/mol indicates that there is no significant effect on the structural stability before and after the mutation, i.e., these amino acids play little roles on the structural stability.

During the EAS, our CAS data showed that the sites at Pro441, Ile442, Asp443, Asn444, Asp446, Ile447, Thr448, and Phe450 had an energy of >0.5 Kcal/mol after mutation to Ala (Figure 5A), suggesting that when these amino acids were mutated, conformational changes of the entire molecule occurred and thereby that the antibody-polypeptide interaction mechanism changed, implying that the amino acids at these sites play key roles in stabilizing the Ab42-pCFH complex.

As shown in Figure 5B, the area under the curve (AUC), as an important pharmacokinetic parameter, represents the bioavailability of the drug (the extent to which the drug is absorbed and utilized in the human body); the larger the AUC, the higher the bioavailability, and *vice versa*.

Preprints (www.preprints.org) | NOT PEER-REVIEWED | Posted: 28 December 2018 doi:10.20944/preprints201812.0336.v1

Figure 5B shows that the AUCs after the alanine mutations of Pro441, Ile442, Asp443, Asn444, Ile447, and Thr448 decreased, respectively, indicating that the amino acids at these sites play important roles in the bioavailability of the protein. Compared with the original CAS data, the results of experimental Ala mutations of PRO441, ILE442, ASP-443, ASN444, ILE447, and THR448 were confirmatory.

However, we also noticed that the results of alanine scanning are not completely consistent with the results of residue decomposition calculated by MM-PBSA, especially for the ASP446, and the main reason may be that the analysis of the residue energy decomposition was obtained in a single run, and it did not change the molecular structure. The contribution of an amino acid to the binding free energy reflects its importance in the complex structure during the alanine scanning process in both CAS and EAS, and when mutated, it not only has a structurally complex effect on the original site but also influence the amino acids around it. In general, our data indicated that the six amino acids PRO441, ILE442, ASP-443, Asn444, Ile447, and Thr448 are the key amino acids for the formation of a stable complex.

Distance monitoring of key amino acids

In order to find out the specific bonds between the key amino acids in the structure of Ab42-pCFH complex, this study also investigated the distance changes between several pairs of amino acids, through which pCFH interacts with Ab42 by hydrogen bond formation, and the amino acid distance changing with time were calculated.

As shown in Table 2, the amino acids on Ab42 interacting with pCFH are located

 doi:10.20944/preprints201812.0336.v1

in the CDR of the antibody, while the key amino acids on the polypeptide (Figure 6B) are Pro441, Ile442, Asp443, Asn444, Ile447, and Thr448, which form hydrogen bonds with the amino acids Tyr315, Ser100, Gly33, and Tyr53 on the CDR of Ab42 respectively. The relevant distance for pCFH is also very stable (Figure 6), implying the stability of the CDR structure. As shown in Figure 6B, the decomposition energy of these amino acid residues in the CDR are negative too, suggesting that the amino acids at these sites contribute significantly to the antigen-antibody binding.

Conclusions

Revealing the details of antigen-antibody interactions and identifying the important amino acid sites (epitopes) through which an antibody interacts with an antigen are critical for the development of an antibody drug. In order to understand the mechanism of interaction between human anti-CFH antibody Ab42 and its target pCFH, the present study has used computational simulation methods, such as homology modeling, molecular docking, MD simulation, and CAS, to study the interaction between Ab42 and pCFH.

The amino acid energy contributions obtained from both the MM-PBSA calculation and the CAS were used in our study to describe the key amino acids of the antigen-antibody interaction, and the results indicated that the mechanisms of interaction between Ab42 and pCFH are mainly hydrogen bond formation and hydrophobic interaction between the amino acids Tyr315, Ser100, Gly33, and Tyr53 on the CDR of Ab42 and the amino acids Pro441, Ile442, Asp443, Asn444, Ile447,

Preprints (www.preprints.org) | NOT PEER-REVIEWED | Posted: 28 December 2018 doi:10.20944/preprints201812.0336.v1

and Thr448 on the pCFH. Finally, all the computational results were verified by the EAS method. As a fully natural human antibody, Ab42 can be further developed into anti-tumor drugs without the concern of invoking immune rejections.

In summary, the present study has important guiding significance not only for the development of Ab4 into anti-tumor drugs but also for the investigation of other relevant antibody-antigen interactions.

Materials and Methods

Structural optimization

The structure of CFH polypeptide was retrieved from the PDB database (PDB_ID: 5EA0)[1]. The Dmol3 quantum chemistry calculation in Discovery Studio software[17] was then applied, with the quantum chemical optimization setting at the density functional theory B3LYP method[12] for optimization, the maximum SCF cycle setting at 300, and the calculated non-bond interaction value setting at 14 angstroms, respectively.

The human antibody Ab42, isolated from our laboratory, is a Fab antibody with 217 amino acids in the heavy chain and 219 amino acids in the light chain. According to the IMGT numbering scheme, The CDR of Ab42 was defined as the following: H-CDR1 (amino acids 26-33), H-CDR2 (amino acids 51-58), H-CDR3 (amino acids 97-108), L-CDR1 (amino acids 244-255), L-CDR2 (amino acids 273-275), and L-CDR3 (amino acids 312-320).

The 3D structure of Ab42 was established using the homology modeling

Preprints (www.preprints.org) | NOT PEER-REVIEWED | Posted: 28 December 2018 doi:10.20944/preprints201812.0336.v1

method[17,18]. DS_Model Antibodies module in the Discovery Studio v4.5 (DS45) package was applied, and the antibody CDRs were optimized using the Model Antibody Loops program. Finally, the charmm27 force field was used in the GBSW solvent model, and the energy minimization (EM) was performed on the DS_Charmm module in DS45. The final convergence was lower than 0.4184 kJ/(mol·nm), and the output structure was the initial structure for molecular docking calculation.

Molecular docking

The molecular docking of pCFH with Ab42 was performed using the ZDock[19,20] module under the Discovery Studio platform. The pCFH and Ab42 molecules were assigned to the all-atom Charmm27 force field[21], first using the steepest descent (SD) method to optimize 1000 steps and then using the conjugate gradient (CG) method, to optimize until the whole system convergence criterion reaching 0.4184 kJ/(mol·nm), with pCFH as the ligand, Ab42 as the receptor, and the antibody CDR defined as the binding region.

The RMSD Cutoff and the Interface Cutoff were set to 6 and 9 angstroms respectively. All the docking poses obtained were scored by ZRank[22], and the highest scored Poses docking conformation was selected for the RDock[23] program. The simulated annealing method was used to reconstruct the docking compound, and the RDock optimization parameters were as follows: Generalized Born with a simple Switching (GBSW), Charmm force field, and dielectric constant 4.0.

MD simulations

MD simulations were peformed to fully optimize the conformation of the

Preprints (www.preprints.org) | NOT PEER-REVIEWED | Posted: 28 December 2018 doi:10.20944/preprints201812.0336.v1

complex. The MD trace was also used to calculate the MM-PBSA[24,25] binding free energy and select the dominant conformation for further analysis of the virtual mutation. The MD was run using the Gromacs 5.1.2 software package[26,27], and the initial model was dissolved in a cube box containing SPC/E water molecules; the system was assigned to the Amber 99sb force field[28]. The entire system was balanced by addition of neutral ions under the Genion program in the Gromacs package.

Before the final production of MD, a 500-step SD optimization of protein molecules in the system was performed to eliminate the positional conflicts from unreasonable van der Waals force, and then a 2 ns position-restricted MD simulation was performed with NVT and NPT[11] ensemble separately.

Finally, a 100 ns unrestricted MD simulation was performed at 300K, with atmospheric NPT ensemble, and under periodic boundary conditions. All the bond lengths were limited by the LINCS algorithm[18], and the electrostatic interactions were calculated using the Particle Mesh Ewald (PME) summation scheme[29]. The time step was set at 2 fs, and the conformations were stored every 20 ps, with each MD trajectory file containing 1,000 conformations.

In the MD simulations, we mainly used the RMSD of backbone to examine whether the system reaches its equilibrium and used the cluster analysis to obtain the representative conformation after the system achieving balance. All of the Gromacs MD simulation jobs were performed on the high performance computing platform of Jinan University.

Preprints (www.preprints.org) | NOT PEER-REVIEWED | Posted: 28 December 2018 doi:10.20944/preprints201812.0336.v1

Binding energy calculation by MM-PBSA

A total of 100 conformations were extracted from the equilibrium phase of each MD locus (wild type and mutant), and the g_mmpbsa software package[30] was executed; the binding free energy and residue decomposition of Ab42 and pCFH complexes were calculated using the MM-PBSA method[13,31].

In MM-PBSA, the enthalpy of the system was calculated using the molecular mechanics (MM) method; the contribution of the polar part and non-polar part of the solvent effect to the free energy were determined by solving the Poisson-Boltzmann (PB) equation and calculating the molecular surface area (SA) respectively. The basic principle is shown in a formula as follows:

$$\Delta G_{bind} = \Delta E_{MM} + \Delta\Delta G_{sol} - T\Delta S$$

$$= \Delta E_{MM} + \Delta G_{GB} + \Delta G_{SA} - T\Delta S$$

$$= \Delta E_{vdw} + \Delta E_{ele} + \Delta G_{GB} + \Delta G_{SA} - T\Delta S,$$

where ΔGbind is the binding free energy; ΔEMM is the difference in intramolecular energy under vacuum; ΔΔGsol is the solvation free energy difference; T is the absolute temperature, and ΔS is the entropy change. The ΔEMM can be calculated by MM method; ΔΔGsol is composed of polar solvation free energy difference and non-polar solvation free energy difference. While the polar part was obtained by solving the finite difference PB equation, the non-polar part was fitted by estimating the solvent accessible SA; finally, the TΔS was calculated using the normal mode method.

CAS

Preprints (www.preprints.org) | NOT PEER-REVIEWED | Posted: 28 December 2018 doi:10.20944/preprints201812.0336.v1

Alanine scanning is to mutate an amino acid into alanine, thereby replacing any functional groups on its side chain with a small neutral methyl group that exerts little effect on the protein structure[14]. In this study, the importance of key amino acids was determined by alanine scanning and calculation of the changes in binding free energy before and after the mutation, in order to find the mechanism of interaction between Ab42 and pCFH. The CAS was performed with the Calculate Mutation Energy (Binding) module under the DS platform; the amino acids on the pCFH were mutated into alanine one by one, and the energy differences between the wild type and the mutants in the antigen-antibody complex were determined subsequently.

The GBIM (Generalized Born with implicit membrane) approximation[32] was used to detect the effect of the solvent, and the electrostatic terms were approximated by the sum of Coulombic interactions and polar contributions to solvation energy. The energy function also contains the van der Waals interaction energy, a side-chain entropy term, and a non-polar surface dependent term.

EAS

Each amino acid in pCFH was mutated into alanine one by one, and, including the wild-type pCFH, a total of 16 polypeptides were synthesizeds for further examination. As shown in Table 1, the peptide purity achieved 99%, and the biotin was coupled for labeling. The ELISA was performed as follows: an ELISA plate was coated with 20 μg/ml streptavidin coating solution (100 μl/well). The plate was incubated overnight at 4 °C, washed with PBST (PBS containing 0.1% Tween 20), and then blocked with PBS containing 5% goat serum at 37 °C for 2 hours. After

 doi:10.20944/preprints201812.0336.v1

washing with PBST, 20 μg/ml of each polypeptide was added and incubated at 37 °C for 1 hour. After washing with PBST, the antibody was added and incubated at 37 °C for 1 hour, and the secondary antibody, horseradish peroxidase-labeled goat anti-human IgG (H+L), was applied. After incubation for another 30 minutes, 100 μl of TMB color developer was added, and the OD values were read at the wavelength of 450 nm.

Acknowledgements

The work was supported by the Guangdong Innovative and Entrepreneurial Research Team Program (No. 2013Y113), National Natural Science Foundations (No. 31400795), Pearl River S&T Nova Program of Guangzhou (No. 201506010097), Opening Fund of Guangdong Provincial Key Laboratory of Computational Science (No. 2016004), Operating Fund of Guangdong Provincial Key Laboratory of Bioengineering Medicine (NO.2014B030301050), Zhuhai Innovative and Entrepreneurial Research Team Program (No. ZH01110405160015PWC), National Basic Research Program of China (973 Program) (No. 2015CB553706).

Conflicts of Interest

The authors declare there is no conflicts of interest regarding the publication of this paper.

References

1. Bushey, R.T.; Moody, M.A.; Nicely, N.L.; Haynes, B.F.; Alam, S.M.; Keir, S.T.; Bentley, R.C.; Roy Choudhury, K.; Gottlin, E.B.; Campa, M.J., et al. A Therapeutic Antibody for Cancer, Derived from Single Human B Cells. *Cell Rep* **2016**, *15*, 1505-1513, doi:10.1016/j.celrep.2016.04.038.
2. Herbert, A.P.; Kavanagh, D.; Johansson, C.; Morgan, H.P.; Blaum, B.S.; Hannan, J.P.; Barlow, P.N.; Uhrin, D. Structural and functional characterization of the product of disease-related factor H gene conversion. *Biochemistry* **2012**, *51*, 1874-1884, doi:10.1021/bi201689j.
3. Amornsiripanitch, N.; Hong, S.; Campa, M.J.; Frank, M.M.; Gottlin, E.B.; Patz, E.F., Jr. Complement factor H autoantibodies are associated with early stage NSCLC. *Clinical cancer research : an official journal of the American Association for Cancer Research* **2010**, *16*, 3226-3231, doi:10.1158/1078-0432.CCR-10-0321.
4. Kajander, T.; Lehtinen, M.J.; Hyvarinen, S.; Bhattacharjee, A.; Leung, E.; Isenman, D.E.; Meri, S.; Goldman, A.; Jokiranta, T.S. Dual interaction of factor H with C3d and glycosaminoglycans in host-nonhost discrimination by complement. *Proc Natl Acad Sci U S A* **2011**, *108*, 2897-2902, doi:10.1073/pnas.1017087108.
5. Ferreira, V.P.; Pangburn, M.K.; Cortes, C. Complement control protein factor H: the good, the bad, and the inadequate. *Mol Immunol* **2010**, *47*, 2187-2197, doi:10.1016/j.molimm.2010.05.007.
6. Campa, M.J.; Gottlin, E.B.; Bushey, R.T.; Patz, E.F., Jr. Complement Factor H Antibodies from Lung Cancer Patients Induce Complement-Dependent Lysis of Tumor Cells, Suggesting a Novel Immunotherapeutic Strategy. *Cancer Immunol Res* **2015**, *3*, 1325-1332, doi:10.1158/2326-6066.CIR-15-0122.
7. Hofer, J.; Giner, T.; Jozsi, M. Complement factor H-antibody-associated hemolytic uremic syndrome: pathogenesis, clinical presentation, and treatment. *Semin Thromb Hemost* **2014**, *40*, 431-443, doi:10.1055/s-0034-1375297.
8. Liao, H.X.; Levesque, M.C.; Nagel, A.; Dixon, A.; Zhang, R.; Walter, E.; Parks, R.; Whitesides, J.; Marshall, D.J.; Hwang, K.K., et al. High-throughput isolation of immunoglobulin genes from single human B cells and expression as monoclonal antibodies. *J Virol Methods* **2009**, *158*, 171-179, doi:10.1016/j.jviromet.2009.02.014.
9. Tonelli, M.; Boido, V.; Colla, P.; Loddo, R.; Posocco, P.; Paneni, M.S.; Fermeglia, M.; Pricl, S. Pharmacophore modeling, resistant mutant isolation, docking, and MM-PBSA analysis: Combined experimental/computer-assisted approaches to identify new inhibitors of the bovine viral diarrhea virus (BVDV). *Bioorganic & medicinal chemistry* **2010**, *18*, 2304-2316, doi:10.1016/j.bmc.2010.01.058.
10. Luo, Q.; Zhang, C.; Miao, L.; Zhang, D.; Bai, Y.; Hou, C.; Liu, J.; Yan, F.; Mu, Y.; Luo, G. Triple mutated antibody scFv2F3 with high GPx activity: insights from MD, docking, MDFE, and MM-PBSA simulation. *Amino Acids* **2013**, *44*, 1009-1019, doi:10.1007/s00726-012-1435-3.
11. Zhang, D.; Chen, C.F.; Zhao, B.B.; Gong, L.L.; Jin, W.J.; Liu, J.J.; Wang, J.F.; Wang, T.T.; Yuan, X.H.; He, Y.W. A novel antibody humanization method based on epitopes scanning and molecular dynamics simulation. *PLoS One* **2013**, *8*, e80636, doi:10.1371/journal.pone.0080636.
12. Yang, Z.; Wu, X.; Yang, G.; Zu, Y.; Zhou, L. Understanding the Chiral Recognitions between Neuraminidases and Inhibitors: Studies with DFT, Docking and MD Methods. *International*

Journal of Quantum Chemistry **2011**, *112*, 909-921.

13. Jiayi, R.; Zhiwei, Y.; Nianjue, Z.; Junqi, L.; Chunlong, Y.; Shujian, L.; Bing, Y.; Junqing, H.; Huaxin, L.; Xiaohui, Y., et al. Effect of ForceFields and Water Models of EGFRvIII (scFv) Complex by Molecular Dynamics Simulation, MM-PBSA Calculation, and ITC Experiment. *Chem J Chinese Universities* **2017**, *38*, 2070-2076.
14. Martins, S.A.; Perez, M.A.; Moreira, I.S.; Sousa, S.F.; Ramos, M.J.; Fernandes, P.A. Computational Alanine Scanning Mutagenesis: MM-PBSA vs TI. *Journal of chemical theory and computation* **2013**, *9*, 1311-1319, doi:10.1021/ct4000372.
15. Liu, X.; Peng, L.; Zhou, Y.; Zhang, Y.; Zhang, J.Z.H. Computational Alanine Scanning with Interaction Entropy for Protein-Ligand Binding Free Energies. *Journal of chemical theory and computation* **2018**, *14*, 1772-1780, doi:10.1021/acs.jctc.7b01295.
16. Gao, M.; Zhang, F.; Zhu, Y.; Gao, L.; Jiang, Y.; Luo, Y.; Zhuang, F.; Mao, Z.; Mao, J. Alanine scanning mutagenesis of SP70 epitope in characterizing speciesspecific antibodies induced by enterovirus 71based antigens. *Mol Med Rep* **2018**, *17*, 1006-1014, doi:10.3892/mmr.2017.7992.
17. Yuan, X.; Qu, Z.; Wu, X.; Wang, Y.; Wei, F.; Zhang, H.; Liu, L.; Yang, Z. Homology Modeling and Evolution Trace Analysis of Human Adenovirus Type 3 Hexon. *Chem J Chinese Universities* **2009**, *30*.
18. Yuan, X.H.; Wang, Y.C.; Jin, W.J.; Zhao, B.B.; Chen, C.F.; Yang, J.; Wang, J.F.; Guo, Y.Y.; Liu, J.J.; Zhang, D., et al. Structure-based high-throughput epitope analysis of hexon proteins in B and C species human adenoviruses (HAdVs). *PLoS One* **2012**, *7*, e32938, doi:10.1371/journal.pone.0032938.
19. Yang, Z.; Wu, F.; Yuan, X.; Zhang, S. *Molecular interactions of GABA analogues against the α+β-interface of GABAA receptor: Docking and molecular dynamics studies*; 2015; Vol. 10, pp. 811-822.
20. Wiehe, K.; Pierce, B.; Tong, W.W.; Hwang, H.; Mintseris, J.; Weng, Z. The performance of ZDOCK and ZRANK in rounds 6-11 of CAPRI. *Proteins* **2007**, *69*, 719-725, doi:10.1002/prot.21747.
21. Sapay, N.; Tieleman, D.P. Combination of the CHARMM27 force field with united-atom lipid force fields. *Journal of computational chemistry* **2011**, *32*, 1400-1410, doi:10.1002/jcc.21726.
22. Pierce, B.; Weng, Z. ZRANK: reranking protein docking predictions with an optimized energy function. *Proteins* **2007**, *67*, 1078-1086, doi:10.1002/prot.21373.
23. Li, L.; Chen, R.; Weng, Z. RDOCK: refinement of rigid-body protein docking predictions. *Proteins* **2003**, *53*, 693-707, doi:10.1002/prot.10460.
24. Kuhn, B.; Gerber, P.; Schulz-Gasch, T.; Stahl, M. Validation and use of the MM-PBSA approach for drug discovery. *Journal of medicinal chemistry* **2005**, *48*, 4040-4048, doi:10.1021/jm049081q.
25. Wang, J.; Morin, P.; Wang, W.; Kollman, P.A. Use of MM-PBSA in reproducing the binding free energies to HIV-1 RT of TIBO derivatives and predicting the binding mode to HIV-1 RT of efavirenz by docking and MM-PBSA. *J Am Chem Soc* **2001**, *123*, 5221-5230.
26. Van Der Spoel, D.; Lindahl, E.; Hess, B.; Groenhof, G.; Mark, A.E.; Berendsen, H.J. GROMACS: fast, flexible, and free. *Journal of computational chemistry* **2005**, *26*, 1701-1718, doi:10.1002/jcc.20291.
27. Abraham, M.J.; Murtola, T.; Schulz, R.; Páll, S.; Smith, J.C.; Hess, B.; Lindahl, E.

GROMACS: High performance molecular simulations through multi-level parallelism from laptops to supercomputers. *SoftwareX* **2015**, *1–2*, 19-25, doi:http://dx.doi.org/10.1016/j.softx.2015.06.001.

28. Showalter, S.A.; Bruschweiler, R. Validation of Molecular Dynamics Simulations of Biomolecules Using NMR Spin Relaxation as Benchmarks: Application to the AMBER99SB Force Field. *Journal of chemical theory and computation* **2007**, *3*, 961-975, doi:10.1021/ct7000045.
29. Yuan, X.H.; Wang, Y.C.; Qu, Z.Y.; Ren, J.Y.; Wu, X.M.; Wang, J.F. Phylogenetic and structural analysis of major surface proteins hemagglutinin and neuraminidase of novel avian influenza virus A H7N9 from chinese patient. *Chem Res Chinese U* **2013**, *29*, 934-940, doi:10.1007/s40242-013-3200-x.
30. Kumari, R.; Kumar, R.; Lynn, A. g_mmpbsa--a GROMACS tool for high-throughput MM-PBSA calculations. *Journal of chemical information and modeling* **2014**, *54*, 1951-1962, doi:10.1021/ci500020m.
31. Thompson, D.C.; Humblet, C.; Joseph-McCarthy, D. Investigation of MM-PBSA rescoring of docking poses. *Journal of chemical information and modeling* **2008**, *48*, 1081-1091, doi:10.1021/ci700470c.
32. Li, T.; Froeyen, M.; Herdewijn, P. Computational alanine scanning and free energy decomposition for E. coli type I signal peptidase with lipopeptide inhibitor complex. *Journal of molecular graphics & modelling* **2008**, *26*, 813-823, doi:10.1016/j.jmgm.2007.04.007.

 doi:10.20944/preprints201812.0336.v1

Figure Legends

Figure 1. The crystal structure and the structure evaluation of Ab42. (A) the crystal structure of Ab42 with the six CDRs displayed by red, yellow, purple, black, blue, and green spheres respectively; (B) Profile_3D verification result of the Ab42 model with residues exhibiting reasonable folding; (C) the Ramachandran plot analysis shows phi-psi torsion angles of all residues in the structure.

Figure 2. The interaction of Ab 42 with pCFH. (A) atomic surface contact of pCFH with Ab42 CDR; (B) two dimensional diagram of the interaction between pCFH and Ab42, with pCFH displayed by ball and stick and the key residues in CDR displayed by disc presentation.

Figure 3. The RMSD as functions of the Ab42-pCFH MD simulation time. (A) the backbone-atom RMSD of whole Ab42-pCFH structure; (B) the CDR-pCFH RMSD of whole Ab42-pCFH structure

Figure 4. Amino acid energy decomposition of pCFH. The red bar or the blue column indicates the binding energies positive or negative respectively after the mutation.

Figure 5. Results of alanine scanning and experimental alanine mutation. (A) CAS; (B) experimental alanine mutation.

Figure 6. The Key amino acid distance between pCFH and Ab42. (A) pCFH441-L315; (B) pCFH442-L315; (C) pCFH444-H100; (D) pCFH447-H33; (E) pCFH448-H53.

Preprints (www.preprints.org) | NOT PEER-REVIEWED | Posted: 28 December 2018 doi:10.20944/preprints201812.0336.v1

Tables

Table 1. The amino acid sequences for peptide synthesis.

Mutation	Location	Sequence
WT	/	GPPPPIDNGDITSFP
M1	P437	APPPPIDNGDITSFP
M2	P438	GAPPPIDNGDITSFP
M3	P439	GPAPPIDNGDITSFP
M4	P440	GPPAPIDNGDITSFP
M5	P441	GPPPAIDNGDITSFP
M6	P442	GPPPPADNGDITSFP
M7	P443	GPPPPIANGDITSFP
M8	P444	GPPPPIDAGDITSFP
M9	P445	GPPPPIDNADITSFP
M10	P446	GPPPPIDNGAITSFP
M11	P447	GPPPPIDNGDATSFP
M12	P448	GPPPPIDNGDIASFP
M13	P449	GPPPPIDNGDITAFP
M14	P450	GPPPPIDNGDITSAP
M15	P451	GPPPPIDNGDITSFA

Preprints (www.preprints.org) | NOT PEER-REVIEWED | Posted: 28 December 2018 doi:10.20944/preprints201812.0336.v1

Table 2. The hydrogen bonds formed in the docking complex.

Donor	Acceptor
Ab42-A:Gly33:HN	Pep-C:Ile447:O
Ab42-A:Tyr53:HH	Pep-C:Gly445:O
Ab42-A:Tyr53:HH	Pep-C:Gly448:O
Ab42-B:Tyr315:HH	Pep-C:Pro439:O
Pep-C:Ile442:HN	Ab42-B:Tyr315:O
Pep-C:Asn444:HD21	Ab42-A:Ala103:O
Pep-C:Asn444:HD22	Ab42-A:Ser100:O
Pep-C:Ser449:HN	Ab42-A:Leu31:O
Ab42-A:Gly33:HA2	Pep-C:Ile447:O
Ab42-A:Ser52:HB1	Pep-C:Asp446:O
Ab42-A:Ser52:HB2	Pep-C:Asp446:O
Ab42-A:Ala101:HA	Pep-C:Asn444:OD1
Pep-C:Pro441:HA	Ab42-B:Tyr315:O
Pep-C:Thr448:HA	Ab42-A:Leu31:O
Pep-C:Thr448:HB	Ab42-A:Leu31:O
Pep-C:Pro441:HD2	Ab42-B:Tyr315:OH

Preprints (www.preprints.org) | NOT PEER-REVIEWED | Posted: 28 December 2018 doi:10.20944/preprints201812.0336.v1

Table 3. The binding free energy of Ab42-pCFH complexes.

	ΔE_{elec}	ΔE_{vdw}	ΔG_{PB}	ΔG_{SA}	$\Delta G_{binding}$ （kJ/mol）
MD-1	-654.037	-307.427	385.53	-33.061	-608.996±55.221
MD-2	-633.372	-304.203	342.451	-31.608	-626.732±65.203
MD-3	-670.679	-316.711	362.541	-33.403	-658.252±66.766

Preprints (www.preprints.org) | NOT PEER-REVIEWED | Posted: 28 December 2018 doi:10.20944/preprints201812.0336.v1

Figures

Figure 1

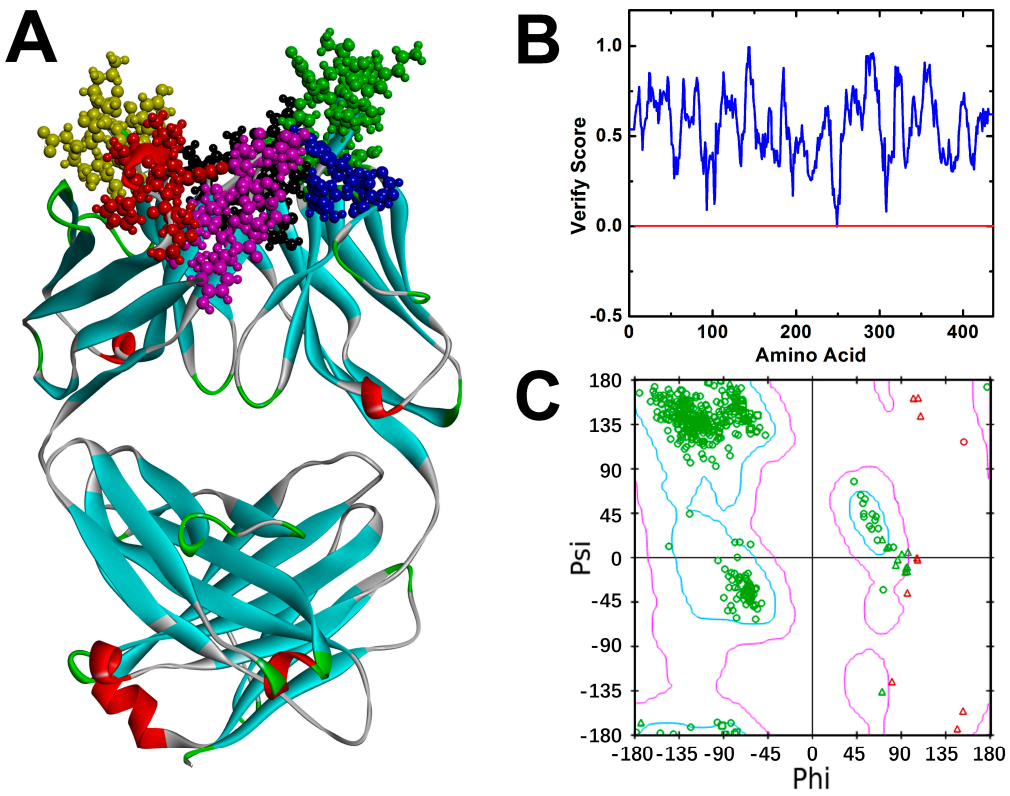

Preprints (www.preprints.org) | NOT PEER-REVIEWED | Posted: 28 December 2018 doi:10.20944/preprints201812.0336.v1

Figure 2

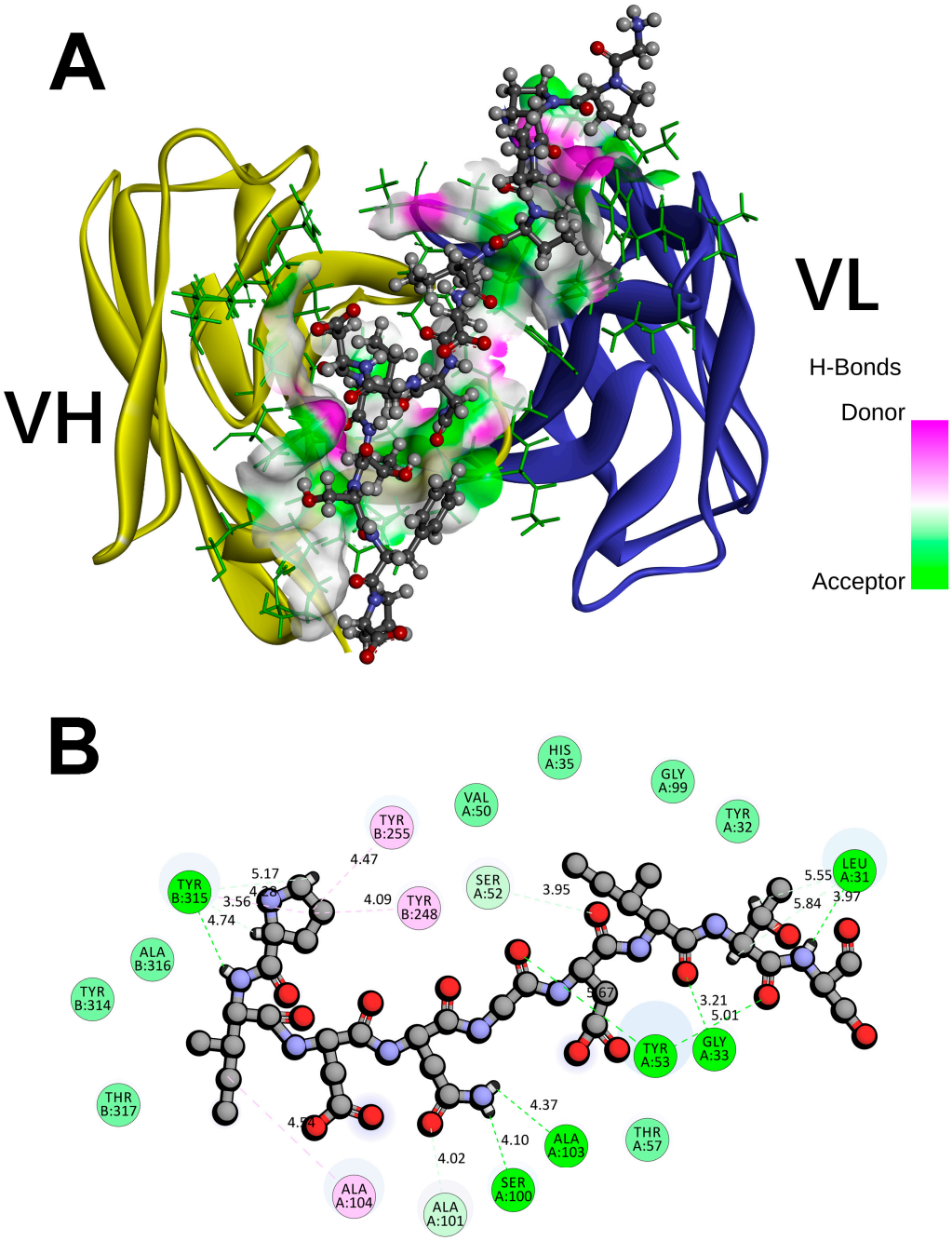

Preprints (www.preprints.org) | NOT PEER-REVIEWED | Posted: 28 December 2018 doi:10.20944/preprints201812.0336.v1

Figure 3

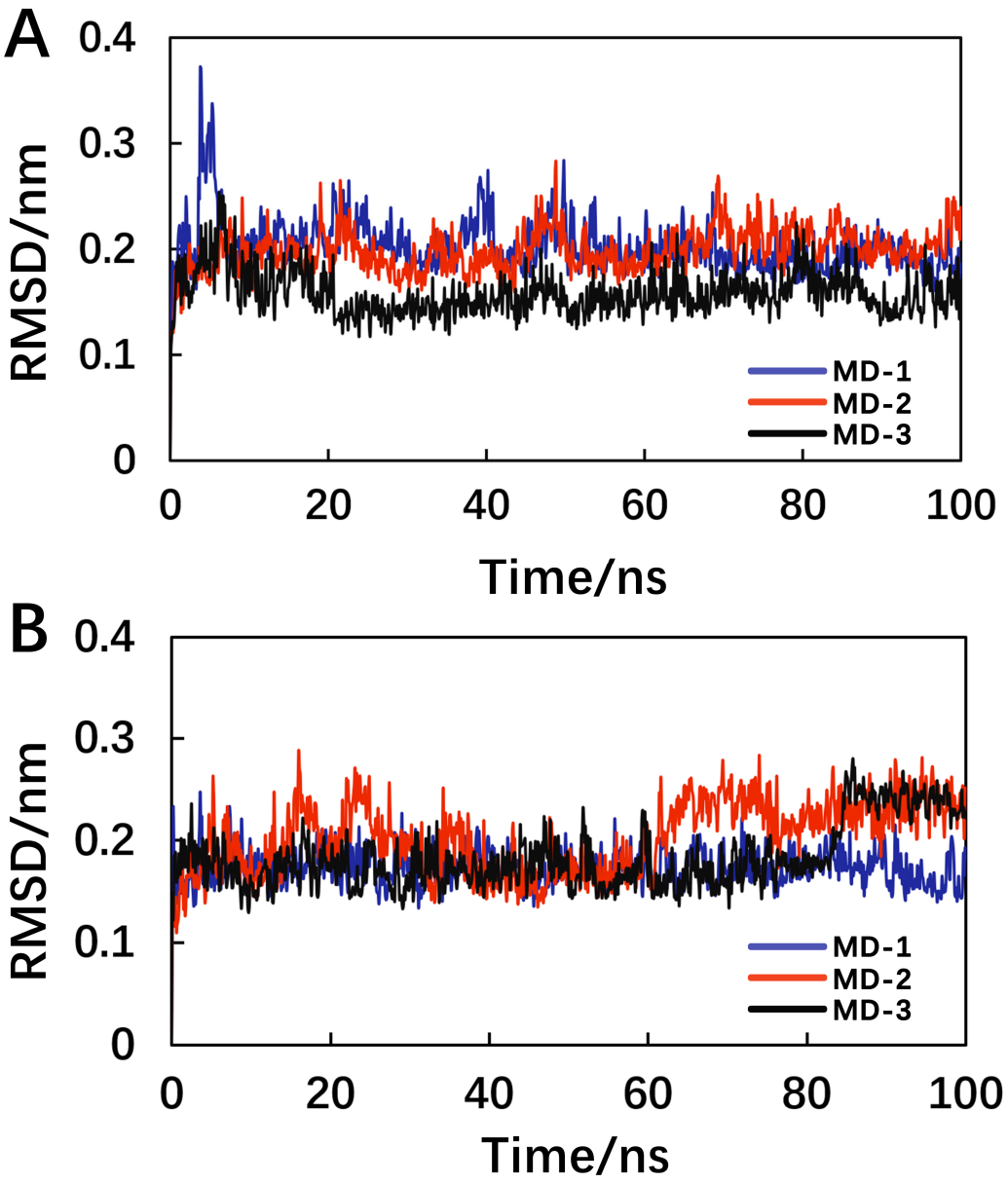

Preprints (www.preprints.org) | NOT PEER-REVIEWED | Posted: 28 December 2018 doi:10.20944/preprints201812.0336.v1

Figure 4

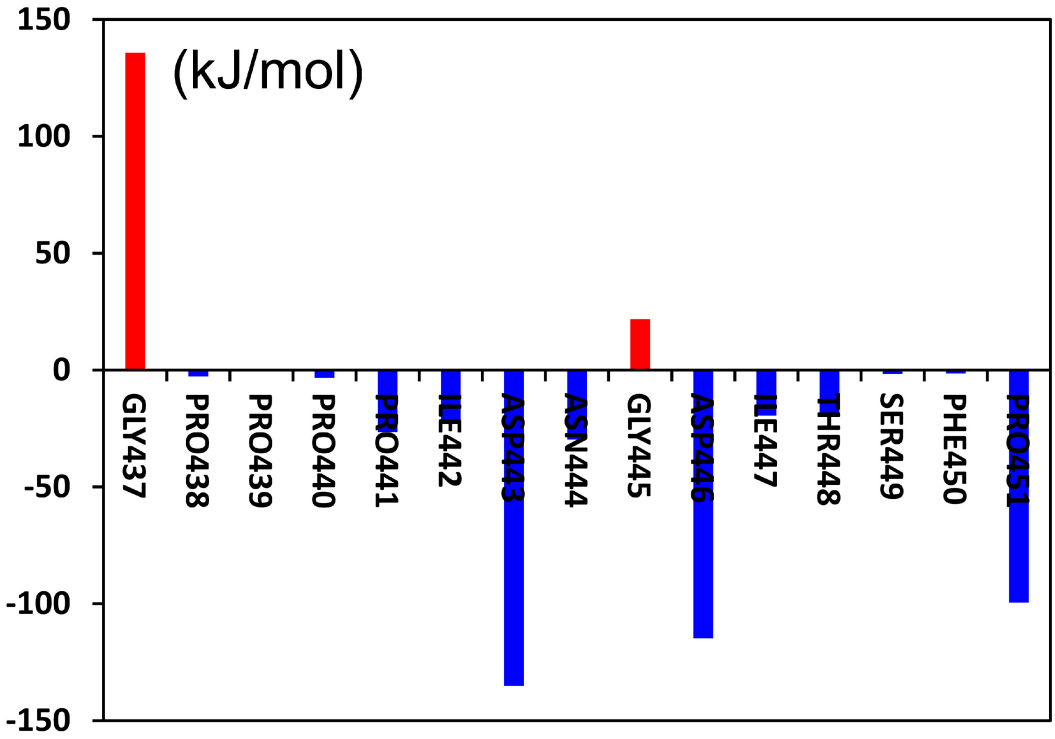

Preprints (www.preprints.org) | NOT PEER-REVIEWED | Posted: 28 December 2018 doi:10.20944/preprints201812.0336.v1

Figure 5

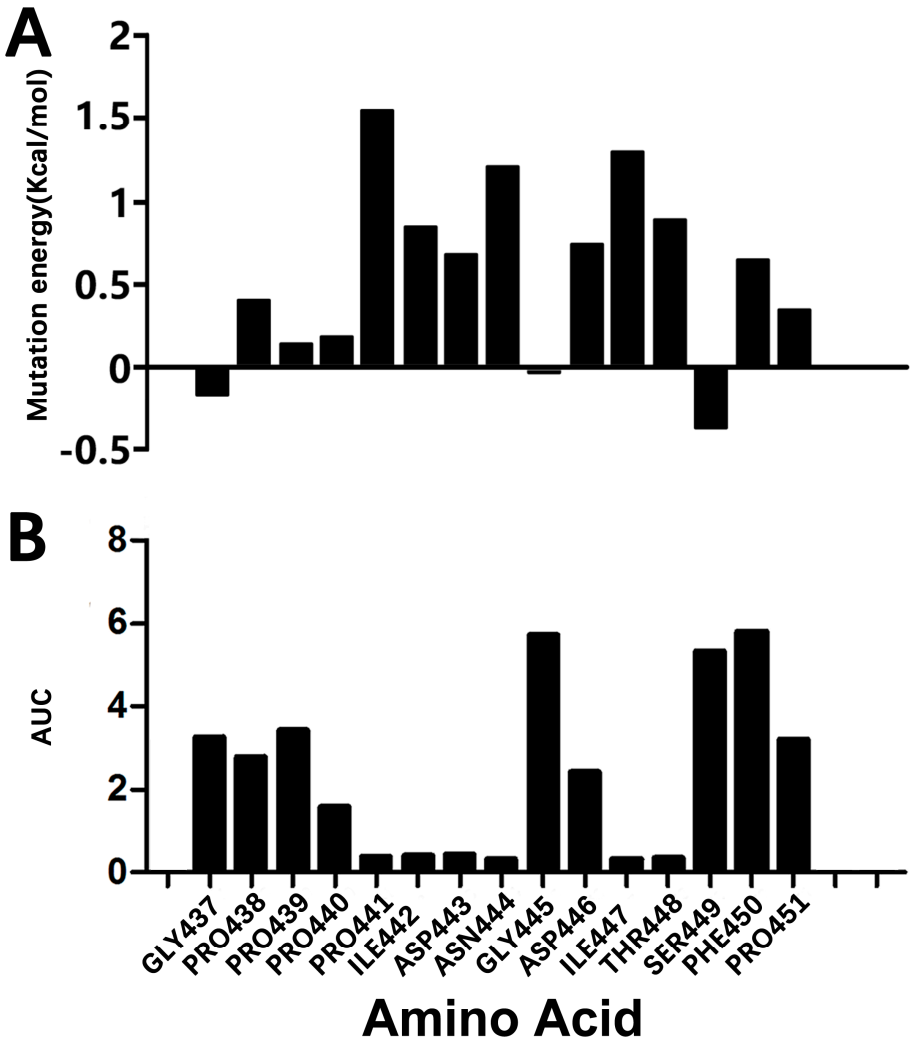

Preprints (www.preprints.org) | NOT PEER-REVIEWED | Posted: 28 December 2018 doi:10.20944/preprints201812.0336.v1

Figure 6